

## Preliminary Results and Analyses of Post-Earthquake Geological Hazards in Jiuzhaigou Based on Airborne LiDAR and Imagery

Jinxing She, Xingxia Zhou, Fei Liu, Duoxiang Cheng, Lu Liao

Technology Service Center of Surveying and Mapping, Sichuan Bureau of Surveying, Mapping and Geoinformation, Chengdu,  
China-shejinxing@qq.com

**KEY WORDS:** Jiuzhaigou scenic spot; Earthquake; Geological disaster; Airborne LiDAR; Optical remote sensing; Remote sensing interpretation

### ABSTRACT:

A magnitude 7.0 earthquake struck Jiuzhaigou County, Sichuan Province at 21:00 on August 8, 2017, and the epicentre was located in the major tourist spot of Jiuzhaigou. This paper describes the surveying and mapping project of post-earthquake hazards regions for the restoration and reconstruction purposes. The earthquake triggered thousands of collapses and landslide disasters, causing severe damage to tourist land scapes and scenic roads such as Jiuzhaigou Panda Sea. The geological hazards of steep mountains and steep slopes and dense vegetation in the scenic area are highly concealed. Traditional susceptibility mapping methods for geological hazard using only airborne images have encountered great difficulties. Aiming to solve this issue, airborne LiDAR and high-resolution images were used jointly to interpret geological disasters in this area. The three-dimensional interpretation signs of disasters are established comprehensively by using optical images and digital elevation models to obtain the distribution characteristics of existing geological hazards, coseismic geological hazards and hidden dangers, which support the restoration and reconstruction of the tourist spots.

### 1. INTRODUCTION

At 21:19:46 on August 8, 2017, a magnitude 7.0 earthquake occurred in Jiuzhaigou County, Sichuan Province, and the epicentre was located in the core scenic spot of Jiuzhaigou (33.20° north latitude, 103.82° east longitude). The earthquake-affected area exceeded 4 000 km<sup>2</sup> (intensity level above and above). Due to the high magnitude, shallow source, and high intensity of the earthquake, and the fragile geological environment in the area, the earthquake triggered thousands of collapses and landslides. The tourist landscape and roads are severely damaged, which had a great impact on the natural landscape and ecological environment of Jiuzhaigou.

The need for geological disaster prevention and ecological environmental protection in the disaster area is urgent. It is difficult to fully discover hidden dangers due to high mountain roads and dense vegetation, and it is difficult to find the hidden dangers of disasters only by artificial ground surveys and group surveys. Satellite imagery are severely blocked by clouds and fog in mountainous areas, and the resolution is relatively low. Airborne LiDAR (Light Detection and Ranging) is used instead, which can penetrate the vegetation through the multiple echos of the LiDAR. Using airborne LiDAR and imagery jointly, provide a promising approach for the identification of geological hazards in vegetation-covered mountains, after removing the influences of vegetation through filtering of the LiDAR point clouds.

In order to complete the restoration and reconstruction of post-earthquake area as soon as possible, the Sichuan Provincial Department of Natural Resources of China launched the "Jiuzhaigou Earthquake Restoration and Reconstruction Survey and Mapping Project for Remote Sensing Prevention and Control". To improve the effectiveness of the investigation, Interferometric Synthetic Aperture Radar (InSAR), airborne LiDAR and imagery are collected in the Jiuzhaigou seismic area, for the monitoring, analysis, assessment. The entire project is

organized by the Sichuan Provincial Bureau of Surveying, Mapping and Geographical Information. Airborne radar data is used to obtain seismic intensity levels of  $\geq 1$  and above, with a cumulative area of 1840 km<sup>2</sup>, among which are Jiuzhaigou tourist area, highways, and population-intensive areas backed by mountains. At 50 km<sup>2</sup>, high-density laser point cloud data was obtained. The other areas were used as general survey areas, and the laser sampling point density was appropriately reduced. In this paper, the interpretation and analysis of geological hazards will be carried out based on the trial production data of 50 km<sup>2</sup> in the core scenic area of Panda Sea.

### 2. STUDY REGION AND DATA

#### 2.1 Study Area

Jiuzhaigou is located in Zhangzha Town, Jiuzhaigou County, Aba Tibetan and Qiang Autonomous Prefecture in the southern part of the Laoshan Mountains in the northwest of Sichuan Province. It is located on the northeast side of Gonggan Ridge in the southern part of Laoshan, with geographical coordinates of 100°30'-104°27'. North latitude 30°35'-34°19'. More than 400 kilometres from Chengdu. The river is a large branch ditch at the source of the Baishui River upstream of the Jialing River. The terrain of Jiuzhaigou Nature Reserve is high in the south and low in the north, the valley is deep, and the height difference is huge. The northern edge of Jiuzhaigou Mouth is only 2,000 meters above sea level, the central peaks and ridges are all above 4,000 meters, the southern edge is more than 4,500 meters, and the main ditch is more than 30 kilometres long. Jiuzhaigou is a world natural heritage, a national key scenic spot, a national tourist attraction, a national nature reserve, a national geopark, and a world biosphere reserve network. A nature reserve whose main purpose is to protect natural landscapes. Jiuzhaigou has become one of the most important tourist destinations in China, with an average annual number of tourists exceeding 5 million. The highest intensity of the earthquake was nine degrees, and the entire scenic area and the surrounding buffer zone were all within the range of eight to nine degree earthquake intensity (Figure 1).

Corresponding author, Xingxia Zhou, Email: 99268265@qq.com

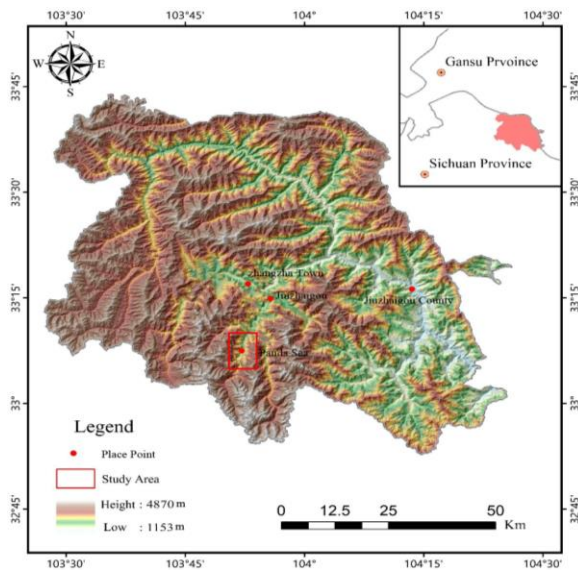


Figure 1. Location distribution of the study area

## 2.2 Advantages of early identification of airborne LiDAR geological hazards

Airborne LiDAR has the technical advantage of penetrating vegetation and reaching the surface. Compared with the geological disaster survey conducted by optical remote sensing technology, high density, high efficiency and high precision are the characteristics of airborne LiDAR measurement technology (Arnone, E., et al., 2016). Compared with traditional optical remote sensing technology, optical remote sensing technology can only obtain two-dimensional spectral feature information, and the spectral information cannot penetrate through vegetation, and it cannot be acquired at night (Bibi, T., et al., 2017). Airborne LiDAR technology can penetrate vegetation (Chang, K.-T., et al., 2007), and the terrain morphological feature information obtained is clear and realistic, which has unique advantages for the identification of landslide disasters. Especially in the southwest alpine canyons and geological disasters at high altitudes, the use of laser point cloud multiple echo technology can effectively identify highly concealed sudden landslide geological disasters under vegetation, and can provide technical support for early identification of geological disasters (Chang, K.-T., et al., 2007). Figure 2 is a comparative study of optical remote sensing interpretation and airborne LiDAR interpretation. From the comparison chart, it can be clearly seen that using the data acquired by the on-board LiDAR technology, after removing the vegetation, using the true surface point cloud to construct a high-precision DEM can clearly see the collapse and accumulation of vegetation underground (Chen, W., et al., 2014).

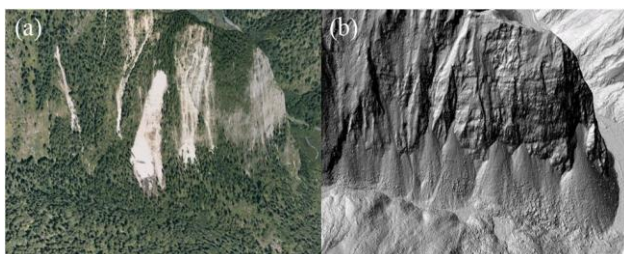


Figure 2. (a) is an optical remote sensing image, (b) is a collapsed deposit found after the vegetation has been removed from the airborne LiDAR data

## 2.3 Airborne LiDAR Data Acquisition

The specific process of acquiring airborne LiDAR data is as follows: (1) Prepared basic geographic information, communication, meteorology, distribution of ground base stations, terrain types of flight areas, types of ground vegetation cover, existing digital ground models, digital orthophotos, etc., and conduct field surveys to obtain relevant data and information; (2) Based on the accuracy index of the results, an aerial photography plan is formulated. In order to ensure the quality and accuracy of point cloud data, a focus analysis is made on the deployment of base stations in areas where high-level remote geological disasters are prone and frequent. Focus on planning and set up mobile base stations in areas that cannot meet the accuracy requirements of point clouds. Secondly, for key areas where the density of point clouds cannot meet the requirements for identification of geological hazards, lower flight heights are used to obtain higher density and higher resolution airborne LiDAR data; (3) Carry out instrument and equipment calibration, obtain whether the point cloud density of the laser scanner meets the technical requirements, and record the number of echoes, scanning angle, scanning frequency and other information. Determine again whether the POS system, ground receiver, and digital camera meet the requirements of the technical specifications of this measurement area. Carry out flight calibration to further eliminate errors and acquire point cloud data in accordance with the established aerial photography plan.

## 2.4 Data pre-processing

First, the on-board GPS data is used for post-difference processing to form high-precision POS result data, and the laser ranging data is combined to generate 3D discrete point cloud data. At the same time, data accuracy and quality inspections are carried out. If the accuracy index requirements are not met, retests are required (Chen, Y., et al., 2018; Chiessi, V., et al., 2010). After passing the preliminary inspection, the denoised filtering, vegetation removal and human-computer interaction processing are performed to obtain the classified point cloud results data. Based on the point cloud classification results, the 1985 national elevation benchmark was used to perform coordinate conversion to generate a digital surface model (DSM) and digital elevation model (DEM). At the same time, a digital orthophoto image (DOM) is generated based on the on-board synchronized images. The data processing uses the industry-leading Finnish TerraSolid software. After operations such as data denoising, filtering, aeronautical zone adjustment, point cloud classification, and construction of DEM, high-precision DEM and DSM data with resolutions better than 0.5 m and 0.2 m DOM image data.

## 2.5 Landslide Interpretation Data

The data used for disaster interpretation include 1: 10000 topographic map data, Jiuzhaigou core scenic area geohazard database data, 1: 50000 regional geological survey data, meteorological and hydrological data, seismic record data, etc. The topographic map data and geographic national condition monitoring data are mainly used for information extraction of geological disasters, including information extraction and disaster assessment of residents, roads, houses, important fields and towns that may be affected by landslides. Historical disaster database data is mainly used for statistical analysis of spatial distribution of disasters. Regional geological survey data is mainly used for structural information extraction such as stratigraphic lithology, stratigraphic boundaries, fault folds, etc., and is used to interpret the disaster-pregnant environment. Meteorological and hydrological data mainly analysed the

relationship between historical rainfall and the spatial distribution of disasters and disaster density, and predict the frequency of disasters. Seismic data are used to analyse the correlation between earthquakes and landslides.

### 3. METHODOLOGY

As shown in Figure 3, our method has three core steps. The first step is to perform digital terrain analysis based on the DEM results generated by airborne LiDAR data to obtain analysis results such as slope, aspect, and mountain shadow. The second step is to construct a three-dimensional interpretation sandbox using DEM and DOM. The third step is to carry out early identification and analysis of geological hazards based on geological knowledge.

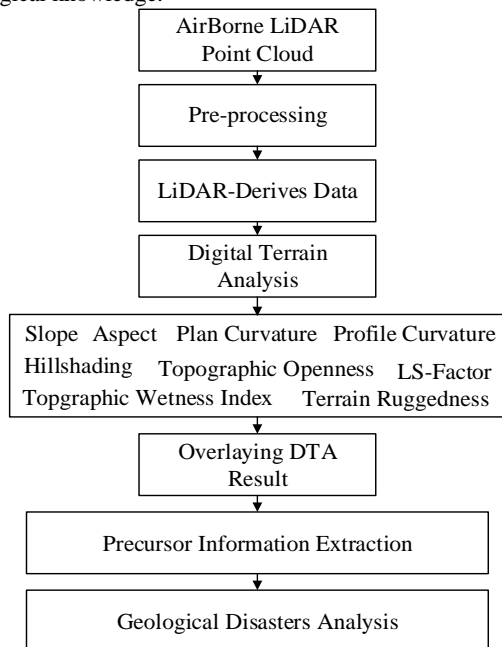


Figure 3. Flowchart of early identification of geological hazards based on airborne LiDAR technology

#### 3.1 An Overview of Geological Hazard Interpretation

This study is based on the development characteristics of geological hazards in the Jiuzhaigou earthquake area. The interpretation work is mainly divided into three levels: (1)The ability of laser radar to "penetrate" the vegetation, mainly to identify adverse geological phenomena that have occurred, such as ancient landslide deposits, Collapsing deposits, and debris flow sources; (2)Co-seismic geological hazards are identified using high-resolution optical images better than 0.2 m. Due to the recent occurrence of disasters induced by the "8.8" Jiuzhaigou earthquake, the characteristics of disaster boundaries are clearly identified in optical images. Mainly small and medium landslide disasters; (3)Comprehensive application of LiDAR and optical imagery to interpret major geological hazards. Although these hidden hazards have not shown signs of instability or obvious deformation during the earthquake, they have the basic geology of large-scale disasters. Conditions and clear threats have potential for further development. It is of great significance to detect and carry out ground review and professional monitoring early.

#### 3.2 Construction of Geological Hazard Interpretation Markers

##### 3.2.1 Landslide interpretation sign

Under the traditional interpretation of the optical remote sensing image, the landslide has a flat shape such as a dustpan shape, a tongue shape, and a pear shape, as well as an irregular slope shape. Landforms such as landslide tongues and landslide cracks (Colkesen, I., et al., 2016; Copons, R. and J. M. Vilaplana, 2008). The back wall of ancient landslides is generally high, and the longitudinal slope of the slope is slow. Sometimes there are trees growing. The size of the landslide is generally large. The surface is flat and the soil is compact. There is no obvious subsidence and unevenness. This work builds a three-dimensional interpretation mark, which is similar to the two-dimensional interpretation mark, but there are differences (Erener, A., et al., 2017). The similarity shows that the landslides are generally similar in shape. The difference is that the airborne LiDAR can not only find the micro topography information more clearly, but also assist the identification of the landslide and the determination of the boundary. There are landslide interpretation signs identified in this work, as shown in Figure 4. The red arrows are the impact boundaries of the disaster.

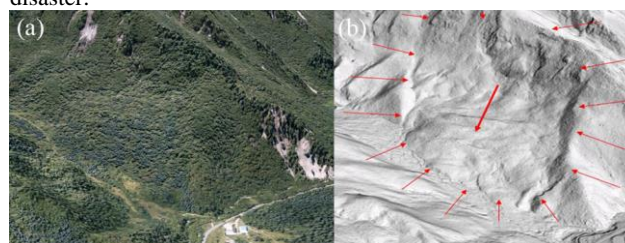


Figure 4. (a) is an optical remote sensing image, (b) is an ancient landslide body found after removing vegetation from airborne LiDAR data

##### 3.2.2 Collapse Interpretation Sign

The interpretation signs of collapse are divided into two types: interpretation signs of collapse deposits and dangerous rock masses. Common collapses occur mostly on cliffs, steep walls, or uneven rock blocks. Through the overlay analysis of the airborne LiDAR mountain shadow map and the synchronously acquired optical image, it is impossible to identify the optical image (Fan, X., et al., 2018). On the mountain shadow map, a clear inverted triangular cone can be seen and the surface is relatively smooth as shown in Figure 5. Dangerous rock masses are often located on steep hillsides. The profile of the dangerous rock masses is steeper and slower. From the image, cracks formed by the joints are sometimes seen in the upper periphery of the dangerous rock masses. Sometimes, the cracks can also be seen through the mountain shadow map.

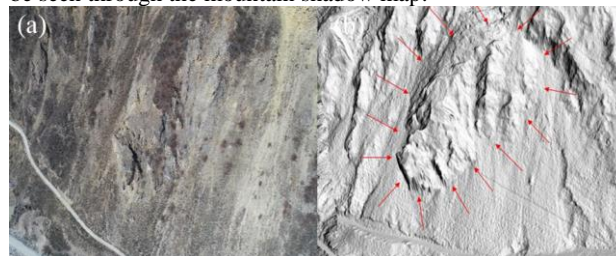


Figure 5. (a) is an optical remote sensing image, (b) is a dangerous rock mass found after removing vegetation from airborne LiDAR data

##### 3.2.3 Debris flow interpretation sign

Through the mountain shadow constructed by the airborne LiDAR, the debris flow ditch can clearly see the source area, circulation area and accumulation area. Among them, the slope of the source area is steep and the weathering of the rocks is

serious. On the mountain shadow map, a large number of loose solid deposits under the vegetation can be clearly seen. Some of these deposits are landslide deposits, and some are collapse deposits. They usually have obvious boundaries. The surface is smooth and has an inverted cone shape (Florham, J. L., et al., 2013). The circulation area is generally the ditch bed of the debris flow ditch, which is in the shape of a straight or curved strip (Guzzetti, F., et al., 1999). The longitudinal slope is slower than the source area but steeper than the accumulation area. The accumulation area is located at the exit of the valley, and the longitudinal slope is gentle and fan-shaped, as shown in Figure 6.

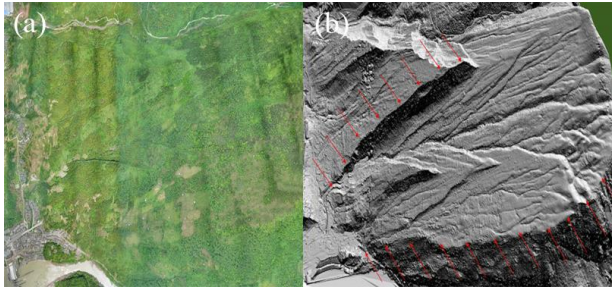


Figure 6. (a) is an optical remote sensing image, (b) is a debris flow disaster found after removing vegetation from airborne LiDAR data

#### 4. RESULTS

##### 4.1 Interpretation of Major Geological Disasters

Hidden dangers of major geological disasters refer to those who already have certain conditions for pregnancy, and have certain signs of deformation and direct threats, including population, important markets, towns, roads, villages, etc., but these threats are not triggered and are called potential geological disasters Hidden danger. Such disasters often have the characteristics of high distribution location, strong vegetation cover, concealment, large scale, and strong damage in mountain areas. Traditional geological survey methods and group survey and group prevention are difficult to find. The main purpose of using airborne LiDAR technology this time is to solve the difficult problem that the traditional optical remote sensing technology cannot penetrate the vegetation in the Jiuzhaigou area to discover the hidden dangers of geological disasters. Through denoising filtering and manual intervention to remove the impact of vegetation, visual interpretation and comprehensive expert judgment methods were used to interpret 83 disaster points with hidden dangers, including 57 collapsed dangerous rock masses, 7 unstable slopes, and debris flow ditch. 19 places. The distribution locations are shown in Figure 7.

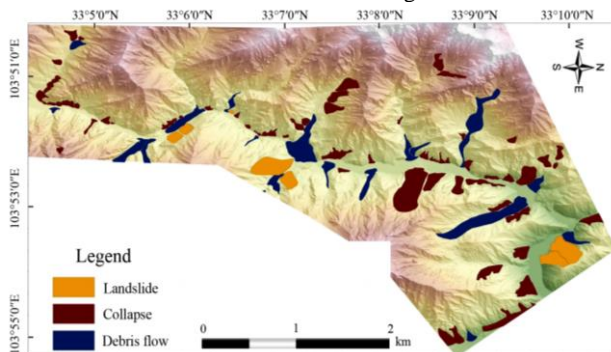


Figure 7. Interpretation of typical debris flow under DEM by airborne LiDAR

##### 4.2 Relationship between identified disaster hazards and slope aspect

Comprehensive use of airborne LiDAR technology and optical remote sensing image interpretation technology to statistically analysed all interpreted geological disasters. As shown in Figure 8, through joint analysis with slope, we find that large landslides are generally distributed in slope areas of 30 ° to 40 °. As the slope further increases, the density of disasters in the same area gradually increases, but the disaster area gradually decrease. This law also indirectly proves that the main types of disasters in the Jiuzhaigou area are small and medium-sized collapses and debris flows.

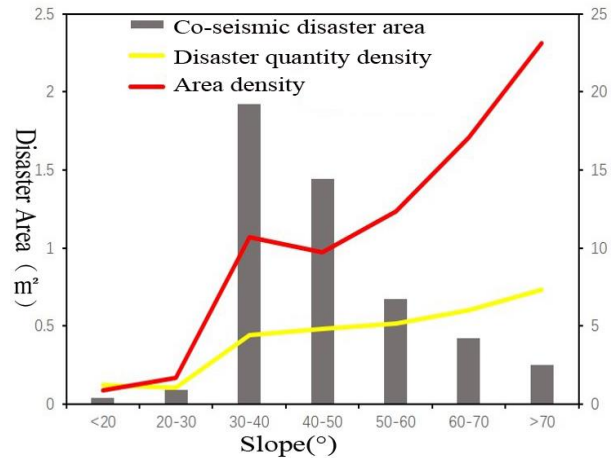


Figure 8 Interpretation of typical debris flow under DEM by airborne LiDAR

##### 4.3 Relationship between disasters and aspect

Comprehensive statistics on the relationship between the number of disasters and the terrain aspect, as shown in Figure 9, through analysis found that most disasters occurred in the southeast direction. Whether it is a collapse or a landslide, the above conclusion is obtained by analyzing the area of the disaster and the aspect map generated by the high-precision DEM. This also reflects the propagation direction of the seismic wave from the side when the earthquake occurred. After confirming the source of the earthquake in the later period, we also clearly proved this view. The source was northwest of our study area.

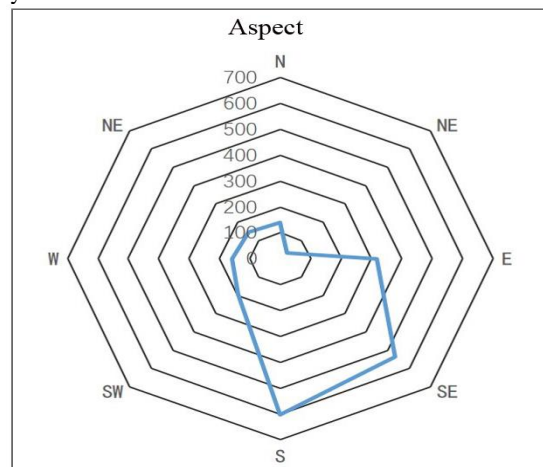


Figure 9. Relationship between geological hazards and aspect

## 5. CONCLUSIONS

This paper introduces the early identification of geological hazards in Jiuzhaigou's high vegetation and complex climatic conditions using the technical advantages of the "penetrable vegetation" of airborne LiDAR technology. Practice has proved that airborne LiDAR technology has certain advantages for early identification of geological hazards. Especially in dense forest areas, by removing vegetation, it is possible to clearly define the precursory information of the landslide such as its outline, morphology, micro-deformation, and tensile cracks. These information are important signs of landslide evolution and further development. Through this work, we also found that airborne LiDAR also has advantages in collapse identification and debris flow identification. The DEM constructed by point clouds has high accuracy, and the collapsed deposits and collapsed rock masses are scanned very clearly. Combined with the three-dimensional interpretation environment to restore the true terrain and landform, it is helpful for the interpreter to accurately determine the collapsed location. In the same way, in the identification of debris flow ditch, the boundary of debris flow ditch and the landslide deposits in the ditch can be accurately defined. These important information are factors that evaluate the danger of debris flow.

Through this study, the research team also clearly found that the simple use of airborne LiDAR technology for early identification of geological hazards has certain limitations. Airborne LiDAR technology can only solve the problem of terrain morphology. To solve the problem of early identification of geological hazards, multi-source data and technologies are needed, including InSAR, LiDAR, multispectral, hyperspectral, and necessary numerical simulation experiments of landslides, collapses, and debris flows combined with ground surveys. The evaluation and analysis of the data can finally achieve the effect.

## ACKNOWLEDGEMENTS

This work was funded by the National key R & D plan (2017YFC0806703), key technology research and application demonstration of unmanned emergency rescue equipment and research on the three-dimensional monitoring technology of pine wood nematode disease(2019YFS0458).

## PREFERENCES

Arnone, E., et al. (2016). "Effect of raster resolution and polygon-conversion algorithm on landslide susceptibility mapping." *Environmental Modelling & Software* 84: 467-481.

Bibi, T., et al. (2017). "Spatio Temporal Detection And Virtual Mapping Of Landslide Using High-Resolution Airborne Laser Altimetry (LiDAR) In Densely Vegetated Areas Of Tropics." *ISPRS - International Archives of the Photogrammetry, Remote Sensing and Spatial Information Sciences XLII-4/W5*: 21-30.

Chang, K.-T., et al. (2007). "Modeling typhoon- and earthquake-induced landslides in a mountainous watershed using logistic regression." *Geomorphology* 89(3-4): 335-347.

Chen, W., et al. (2014). "Forested landslide detection using LiDAR data and the random forest algorithm: A case study of the Three Gorges, China." *Remote Sensing of Environment* 152: 291-301.

Chen, Y., et al. (2018). "Seismological challenges in earthquake hazard reductions: reflections on the 2008 Wenchuan earthquake." *Science Bulletin* 63(17): 1159-1166.

Chiessi, V., et al. (2010). "Geological, geomechanical and geostatistical assessment of rockfall hazard in San Quirico Village (Abruzzo, Italy)." *Geomorphology* 119(3-4): 147-161.

Colkesen, I., et al. (2016). "Susceptibility mapping of shallow landslides using kernel-based Gaussian process, support vector machines and logistic regression." *Journal of African Earth Sciences* 118: 53-64.

Copons, R. and J. M. Vilaplana (2008). "Rockfall susceptibility zoning at a large scale: From geomorphological inventory to preliminary land use planning." *Engineering Geology* 102(3-4): 142-151.

Erener, A., et al. (2017). "Analysis of training sample selection strategies for regression-based quantitative landslide susceptibility mapping methods." *Computers & Geosciences* 104: 62-74.

Fan, X., et al. (2018). "What we have learned from the 2008 Wenchuan Earthquake and its aftermath: A decade of research and challenges." *Engineering Geology* 241: 25-32.

Florsheim, J. L., et al. (2013). "Basin-scale and travertine dam-scale controls on fluvial travertine, Jiuzhaigou, southwestern China." *Geomorphology* 180-181: 267-280.

Guzzetti, F., et al. (1999). "Landslide hazard evaluation: a review of current techniques and their application in a multi-scale study, Central Italy." *Geomorphology* 31(1): 181-216.